# Processing and sintering of sodium-potasium niobate–based thick films

Hugo Mercier[1,2,3], Barbara Malič[1,2], Hana Uršič[1], Danjela Kuscer[1], Franck Levassort[3]

[1]Jožef Stefan Institute, Electronic Ceramics Department, Ljubljana, Slovenia
[2]Jožef Stefan International Postgraduate School, Ljubljana, Slovenia
[3]GREMAN UMR-CNRS 7347, Université de Tours, INSA Centre Val de Loire, Tours, France

**Abstract:** The electrophoretic deposition (EPD) and sintering of $(K_{0.5}Na_{0.5})_{0.99}Sr_{0.005}NbO_3$ (KNNSr) thick films on platinized alumina substrate is reported. We demonstrate that by a two-step deposition-sintering the KNNSr films thicker than 30 μm without defects can be prepared. The effect of the sintering time on structural, microstructural, dielectric and electromechanical characteristics of the KNNSr thick films is discussed. By increasing the sintering time from 2 to 4 hours, the density and the dielectric permittivity of the thick films increased. The unit cell parameters of the perovskite phase decreased which could be related to the formation of polyniobate and volatilization of akalies. Processed KNNSr exhibited promising electromechanical and piezoelectric properties, with a thickness coupling factor up to 35 % and piezoelectric coefficient $d_{33}$ up to 80 pC/N.

**Keywords:** sodium potassium niobate; electrophoretic deposition; thick films, piezoelectric properties; electromechanical properties

# Priprava in sintranje debelih plasti na osnovi natrijevega kalijevega niobata

**Izvleček:** Študirali smo sintranje debelih plasti $(K_{0.5}Na_{0.5})_{0.99}Sr_{0.005}NbO_3$ (KNNSr), ki smo jih na metalizirani korundni podlagi pripravili z metodo elektroforetskega nanosa. Pokazali smo, da z dvostopenjskim nanosom in sintranjem lahko pripravimo plasti KNNSr debelejše od 30 μm in brez defektov. V prispevku poročamo o vplivu časa sintranja plasti KNNSr na njihovo strukturo, mikrostrukturo ter dielektrične in elektromehanske lastnosti. Gostota in dielektrična konstanta plasti KNNSr se poveča s podaljšanjem časa sintranja od 2 na 4 ure, parametri perovskitne osnovne celice pa se zmanjšajo, kar pripisujemo tvorbi sekundarne faze poliniobata in izhajanju alkalijskih oksidov med sintranjem. Plasti KNNSr imejo obetajoče elektromehanske in piezoelektrične lastnosti: povprečni sklopitveni faktor je 35 %, piezoelektrični koeficient $d_{33}$ pa do 80 pC/N.

**Ključne besede:** natrijev kalijev niobat; elektroforetski nanos; debele plasti; piezoelektrične lastnosti; elektromehanske lastnosti

* Corresponding Author's e-mail: hugo.mercier@univ-tours.fr

## 1 Introduction

Piezoelectric energy harvester (PEH) allows the conversion of mechanical energy into electrical energy which can power wireless, self-powered microsystems and macroscale devices [1, 2]. A typical PEH structure is a bimorph cantilever with two layers of piezoelectric material on both sides of a flexible substrate.

Piezoelectric layers of lead-based materials, typically lead zirconate titanate, have been mainly used due to their outstanding piezoelectric properties [3]. However due to lead toxicity and environmental problem there is a need to replace them with environment-benign material. Among the lead-free piezoelectric materials, potassium sodium niobate $((K_{0.5}Na_{0.5})NbO_3$ - KNN) have been extensively studied. The processing of a dense single phase KNN ceramics is challenging, due to the hygroscopic nature of the raw material, the narrow temperature range of sintering, and the volatilization of alkaline species at the processing temperature [4]. Literature reports that addition of 0.5 % Sr, as A-site donor dopant, $((K_{0.5}Na_{0.5})_{0.99}Sr_{0.005}NbO_3$ - KNNSr) improves the density and dielectric/piezoelectric properties of the material ($d_{33} \sim 80$ pC/N, $k_t \sim 0.4$, dielectric permittivity $\sim 500$ and dielectric losses $\sim 0.03$) [4, 5].

Bimorph cantilever PEH have been often prepared by thinning piezoelectric bulk ceramics from a few hundreds to tens of micrometers and consequent gluing of slices [7,8] onto a substrate. This process is complicated and time consuming. Another possibility is to process the thick piezoelectric films directly onto a conductive substrate using thick film technologies. Among them, electrophoretic deposition (EPD) [9] allows the deposition of piezoelectric thick films within a few minutes onto complex-shape substrates. EPD is suitable method for processing a cantilever, since the deposition can be done simultaneously on the top and bottom side of the substrate.

KNN-based thick films have been prepared by EPD using ethanol-, acetone- and water-based suspensions [10–12]. In a previous work, the processing of KNNSr thick films prepared from ethanol-based suspension, and sintered at 1100 °C for 2 hours in air, was reported. The processed thick films were around 25 µm thick and they exhibited a relative density of 75 %, a dielectric constant of 294, dielectric losses of 0.05 at 1 MHz at 20 °C and a $d_{33}$ of 60 pC/N [12].

The lower density of thick films compared to bulk ceramic can be related to the sintering of the thick film in constrained conditions. The clamping of the thick film on the substrate may result in a tensile stress which hindered the densification of the layers [13, 14]. The stresses relax through growth of defects and or/delamination of the thick film from the substrate [15].

In order to improve the density and functional properties of KNN-based thick films, the effect of sintering conditions were studied. It was shown that density of KNN-based material increases with the sintering time [16], but larger time may lead to the formation of larger amount of secondary phases [17]. Sintering of KNN-based ceramics in oxygen atmosphere showed several advantages compared to sintering in air: increased density [18], limited amount of secondary phases [17], reduced oxygen vacancy concentration and improved electromechanical properties [19, 20].

The aim of this work was to process KNNSr thick films on platinized alumina substrate by EPD with final thickness greater than 30 µm. In this case the use of a two steps deposition-sintering process was developed. Moreover the effect of sintering time, i.e., 2 and 4 hours, on the structure, microstructure, dielectric and electromechanical properties of the thick films was studied.

## 2 Experimental

$(K_{0.5}Na_{0.5})_{0.99}Sr_{0.005}NbO_3$ (KNNSr) powder was prepared by solid-state synthesis as described elsewhere [21]. Bulk KNNSr ceramics was prepared by compacting KNNSr powder with a uniaxial press into cylindrical samples, followed by cold isostatically pressing at 200 MPa and sintering at 1120 °C in air with heating and cooling rates of 5 K/min.

The suspension was prepared by mixing 1 vol % of the KNNSr powder in absolute ethanol ($C_2H_5OH$, anhydrous, Carlo Ebra, Italy) with 50 µmol/g poly(acrylic acid-co-maleic acid) (Mw 3.000, 50 wt % water solution, Sigma Aldrich, Germany) and 100 µmol/g n-butylamine (Alfa Aesar, Germany), as detailed in [12].

The substrate acting as a working electrode was prepared by screen-printing platinum paste (Ferro 1192, USA) onto an alumina substrate (A493, Kyocera, Japan). The paste was deposited on a region of 8 x 8 mm and fired at 1200 °C for 1 hour in air. The counter electrode was a platinum disc (thickness of 0.1 mm and diameter of 8 mm).

EPD were performed in a custom-made setup at a constant current density of 1.56 A/cm$^2$ provided by a Keithley 2400 source meter. The layers were deposited either in a single step for 120 s (sample denoted KNNSr-R) or in two steps. In two steps deposition, the first step included the deposition of KNNSr for 60 s, and the presintering of as-deposited layers at 1000 °C for 2 h in oxygen with heating and cooling rate of 2K/min. Samples were denoted KNNSr-L. In the second step, second layers were deposited onto KNNSr-L for 60 s and afterward sintered at 1100 °C in oxygen for 2 hours (sample denoted KNNSr-2h) and 4 hours (sample denoted KNNSr-4h).

The X-ray powder-diffraction data (XRD) were collected in the 2θ range from 20° to 60° in steps of 0.034°, by PANalytical diffractometer (X'Pert PRO MPD, The Netherlands). The phases were identified using the software X-Pert High Score and the PDF-2 database [22]. The unit cell parameters were refined using JANA2006 software, by performing a full pattern matching, assuming a *P1m1* space group. A zero-error shift correction was used to obtain the correct initial position, the background was calculated using a Legendre polynomial and the peak profiles were refined using a pseudo-Voigt function.

The polished cross-sections of the sintered films were analyzed using scanning electron microscopes (SEM, JSM-5800 and JSM 7600F, both JEOL, Japan).

Gold electrodes, with a diameter of 1.5 mm and a thickness of ~100 nm, were sputtered (5 Pascal, Italy) on top of the sintered samples. The capacitance and dielectric losses (tan δ) were measured in the frequency range 10 kHz-1 MHz at room temperature with an impedance spectroscopy analyzer (4192A Hewlett Packard, USA). Samples were poled for 40 min at 120 °C with a DC-electric field of 3 kV/mm. The piezoelectric constants $d_{33}$ were measured with a Berlincourt piezometer (Take Control PM10, Birmingham, UK).

The complex electrical impedance, around the fundamental thickness mode was measured using a vector analyzer (HP4395) and its impedance test kit. A theoretical model, based on the Krimholtz-Leedom-Matthaei (KLM) equivalent electrical circuit [23], delivers the theoretical complex impedance of the thickness mode as a function of the frequency. By fitting the experimental data with the theoretical model, the thickness mode parameters of the KNNSr sintered and poled thick films are deduced. The modeled structure was composed of 3 layers: the alumina substrate; the Pt bottom electrode and the thick piezoelectric film. The top gold electrode was neglected as it was too thin to have a significant effect. The parameters of the inert layers [24] and the thickness of the piezoelectric films are considered as fixed in the model. The following parameters were deduced: the thickness coupling factor $k_t$, the longitudinal wave velocity $v_l$, the dielectric constant at constant strain $\varepsilon_{33}^{S}/\varepsilon_0$ and the tangent of the dielectric loss angle $\delta_e$.

## 3 Results and discussion

### 3.1 Processing of KNNSr thick films

Sample KNNSr-R, deposited in a single step, exhibited defects at its surface, resulting in shortcuts, preventing the electrical measurements, see Figure 1.a. The thickness of the as-deposited layer KNNSr-R was around 60 μm and around 40 μm after sintering. This thickness was presumably above the critical thickness thus defects occurred during the drying and/or the sintering of the thick film [25,26]. In order to process defect-free thick films with final thicknesses above 30 μm, a two steps process was used. A first layer was deposited and pre-sintered (KNNSr-L). KNNSr-L had a deposited yield of 3.5 ± 0.5 mg/cm² and a sintered thickness of 18 ± 5 μm and did not exhibit large defects after its processing (Figure 1.b).

The second layer was deposited on the top of the first one (60 s) and sintered at selected conditions given for KNNSr-2h and KNNSr-4h. The cumulative deposition time for the two layers was the same as for KNNSr-R,
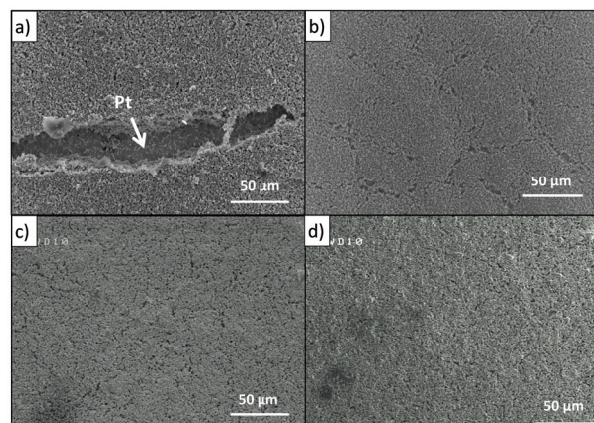


**Figure 1:** SEM image of the surface of sintered KNNSr thick films a) KNNSr-R b) KNNSr-L c) KNNSr-2h and d) KNNSr-4h.

i.e., 120 s. The processed thick films prepared with the described procedure did not exhibit large defects at their surfaces (Figure 1.c and d).

### 3.2 Sintered KNNSr thick films

The XRD patterns of the thick films sintered for 2 (KNNSr-2h) and 4 hours (KNNSr-4h) are presented in Figure 2. Both samples consisted of a main monoclinic perovskite phase indexed as $K_{0.65}Na_{0.35}NbO_3$ (PDF: 77-0038), and a polyniobate phase indexed as $K_{5.75}Nb_{10.85}O_{30}$ (PDF: 38-0297). In addition the diffraction peaks of the top gold electrode and of the platinum bottom electrode were also observed on the diffraction pattern. The formation of the polyniobate phase, which was not identified in the initial powder, may be related to the volatilization and segregation of alkaline species [4].
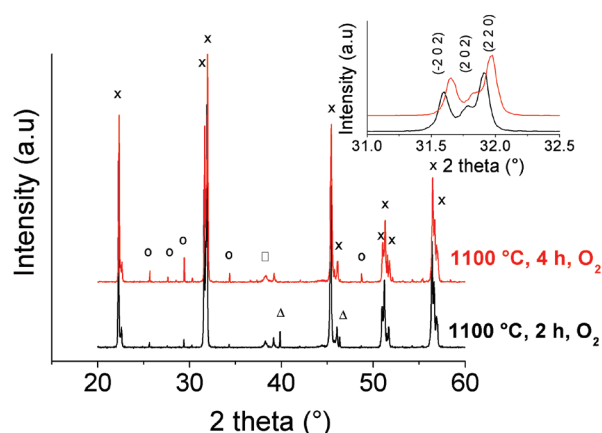


**Figure 2:** XRD patterns of KNNSr thick films sintered at 1100 °C in oxygen for 2 and 4 hours. x: $K_{0.65}Na_{0.35}NbO_3$ (PDF: 77-0038), o: $K_{5.75}Nb_{10.85}O_{30}$ (PDF: 38-0297), Δ: Platinum (PDF:04-0802), □: Gold (PDF: 01-1172).

The calculated cell parameters for the samples KNNSr-2h and KNNSr-4h are presented in Table 1. The calculated unit cell parameters exhibited lower values than the one reported in the literature for bulk ceramics with the same composition [27]. The reduction in the unit cell parameters may be attributed to two phenomena. First phenomenon was the loss of alkali oxides during the sintering. Literature reports that potassium vapor pressure above KNN is greater than sodium one [28,29]. Since potassium ions have a larger radius ($K^+$, 0.164 nm) than sodium ions ($Na^+$, 0.139 nm) the perovskite with K/Na ratio smaller than 1 resulted in a decrease of the unit cell parameters of the perovskite phase [29,30]. In the case of a thick film this phenomenon is expected to be enhanced due the increased area to volume ratio in comparison to bulk ceramic. The second phenomenon was the formation of a polyniobate phase, clearly observed on the XRD spectra. The polyniobate phase had a potassium-rich composition, thus the perovskite phase could have lower potassium content and this again decreased the unit cell parameters of the perovskite phase. On XRD patterns peaks attributed to the polyniobate phase had higher intensity in the samples KNNSr-4h in comparison to KNNSr-2h which indicated the presence of a larger amount of polyniobate phase and may explain the further reduction in the unit cell parameters of KNNSr-4h.

The polished cross-section SEM images of the sintered thick films KNNSr-2h and KNNSr-4h, are presented in Figure 3.a and b, respectively. The microstructure of the samples consisted of micrometers sized pores randomly distributed in a KNNSr particles matrix, see insets Figure 3. Phase composition by EDXS showed that the matrix is a perovskite with K/Na ratio of about 1. Larger grains (see black arrows on the SEM images) had a K/Na ratio greater than 1 and were presumably polyniobate phase. The relative density, estimated from the SEM images were 77 ± 4 % and 87 ± 4 % for KNNSr-2h and KNNSr-4h, respectively. This showed that by increasing the sintering time from 2 to 4 hours, the density of the thick films increased by 10 %. The thickness of KNNSr-2h and KNNSr-4h were 33 and 45 μm, respectively. The discrepancy in the thickness was attributed to the variation in the as-deposited layers thickness, i.e. ± 5μm, for each deposited layer.
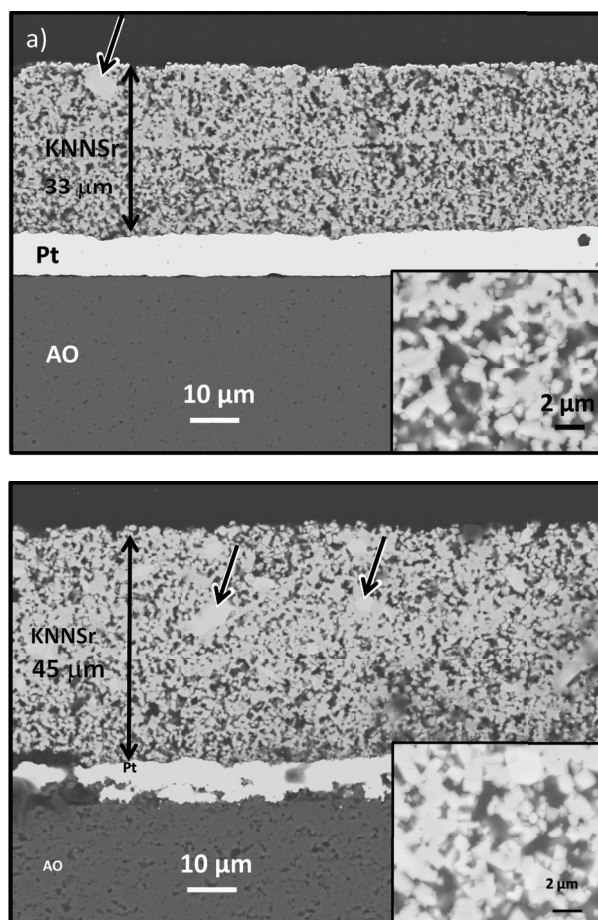


**Figure 3:** Polished cross-section SEM images of KNNSr thick films sintered at 1100 °C in oxygen for a) 2 hours (KNNSr-2h) and b) 4 hours (KNNSr-4h). The insets show KNNSr thick films microstructures at larger magnification; the black arrows show examples of larger grains (polyniobate).

### 3.3 Functional characterizations

The dielectric measurements of the thick films are presented in Figure 4. The permittivity and losses decreased with increasing frequency. Values of KNNSr-4h permittivity and losses are higher than those of KNNSr-2h in the same measured frequency range. The dielectric permittivity and losses at 100 kHz were 230 and 0.04, respec-

**Table 1:** Refined unit cell parameters of the KNNSr thick films sintered at 1100 °C in oxygen for 2 h (KNNsr-2h) and 4 h (KNNSr-4h) and unit cell parameters reported for the KNNSr ceramics.

| Sample | a | b | c | β | V |
|---|---|---|---|---|---|
| | [nm] | [nm] | [nm] | [°] | [nm³] |
| KNNSr-2h | 0.40028(9) | 0.39443(6) | 0.39961(9) | 89.70(2) | 0.06309(4) |
| KNNSr-4h | 0.40016(9) | 0.39431(6) | 0.39946(9) | 89.69 | 0.06303(2) |
| KNNSr bulk [27] | 0.400375 | 0.394596 | 0.399938 | 90.3228 | 0.06318 |
| Estimated error | ± 0.0001 | ± 0.0001 | ± 0.0001 | ± 0.001 | ± 0.00002 |

**Table 2:** Properties of thick piezoelectric films KNNSr-2h, KNNSr-4h, KNNSr bulk ceramic and KNN-based screen printed thick films.

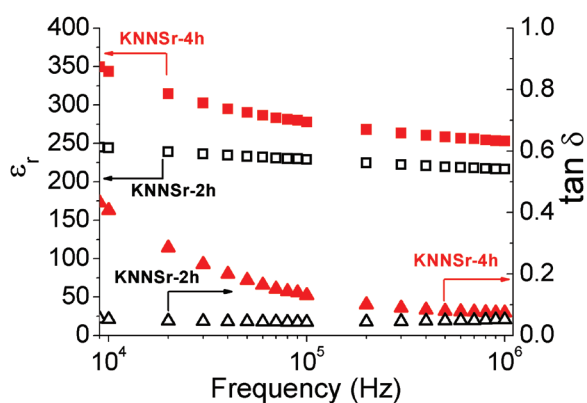| Sample | Thickness | $k_t$ | $\varepsilon_{33S}/\varepsilon_0$ | $\delta_e$ | $d_{33}$ |
|---|---|---|---|---|---|
| | [μm] | [%] | | [%] | [pC/N] |
| KNNSr-2h | 33 | 35 | 155 | 3 | 80 |
| KNNSr-4h | 45 | 32 | 165 | 5 | 80 |
| KNNSr-bulk ceramic 1120 °C, 2 h, air | / | 40 | 300 | 5 | 90 |
| KNN-based screen printed thick films [32] | 43 | 30 | 140 | / | / |



**Figure 4:** Dielectric permittivity (square) and dielectric losses (triangle) of the KNNSr thick films sintered at 1100 °C in oxygen for a) 2 hours (□,△, KNNSr-2h) and b) 4 hours (■,▲, KNNSr-4h).



**Figure 5:** Complex electrical impedance (Re(Z): real part, Im(Z): imaginary part) of KNNSr-2h thick film on platinized alumina substrate as a function of the frequency around fundamental resonance (■: experimental;—: theoretical).

tively, for KNNSr-2h against 280 and 0.13, respectively for KNNSr-4h samples. The increased permittivity may be related to the increased density of the thick film. The increased losses at low frequencies are presumably related to the increased electrical conductivity in the sample. This may be due to the increased amount of secondary phases and/or to the humidity during the dielectric measurement which can strongly impact the dielectric permittivity and losses at low frequencies (under 10 kHz) in strontium doped KNN ceramics [31].

The piezoelectric and electromechanical properties of KNNSr-2h and KNNSr-4h are presented in Table 2. The experimental and theoretical complex impedances of the KNNSr-2h sample are presented in Figure 5, showing the good agreement between the adjusted KLM scheme and the experimental data.

For both KNNSr-2h and KNNSr-4h samples, high $d_{33}$ coefficients around 80 pC/N were obtained. Similar electromechanical properties for KNNSr-2h and KNNSr-4h samples were measured with $k_t$ up to 35 %. Dielectric constant, $k_t$ and $d_{33}$ of the thick films were lower than the one of the processed KNNSr bulk ceramics, which is related to the lower density of the thick films, their deviation from the stoichiometry KNN, and the polyni-
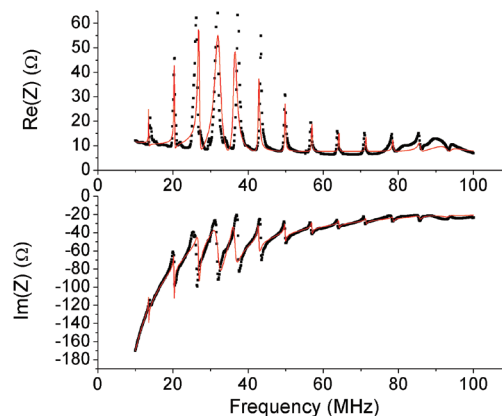
obate phase. The thick films electromechanical properties were similar to values reported in the literature [32]. This demonstrates that the thick films prepared by EPD were at the state of the art in terms of electromechanical properties.

## 4 Summary

KNNSr thick films have been processed by EPD on platinized alumina substrates using a two steps deposition method followed by sintering at 1100 °C in oxygen for 2 and 4 hours. The structural, microstructural, dielectric and electromechanical properties have been reported. The increasing sintering time from 2 to 4 hours leads to higher density, and reduction in unit cell parameters which was related to the formation of a polyniobate phase and the volatilization of alkali oxides. Dielectric constant of the thick film sintered for 4 hours was 280 at 100 kHz and room temperature which is higher value compared to the samples sintered for 2 hours and in agreement with its increased density. The electromechanical performance stayed relatively stable with $k_t$ up to 35 % and $d_{33}$ up to 80 pC/N.

## 5 Acknowledgment

## 6 Literature

1. R.M. Ferdous, A.W. Reza, M.F. Siddiqui, Renewable energy harvesting for wireless sensors using passive RFID tag technology: A review, Renew. Sustain. Energy Rev. 58 (2016) 1114–1128.

2. H. Kim, Y. Tadesse, S. Priya, Piezoelectric energy harvesting, in: S. Priya, D.J. Inman (Eds.), Springer US (2009) 3–39.

3. M.-G. Kang, W.-S. Jung, C.-Y. Kang, S.-J. Yoon, Recent Progress on PZT Based Piezoelectric Energy Harvesting Technologies, Actuators. 5 (2016).

4. B. Malič, J. Koruza, J. Hreščak, J. Bernard, K. Wang, J.G. Fisher, A. Benčan, Sintering of lead-free piezoelectric sodium potassium niobate ceramics, Materials (Basel). 8 (2015) 8117–8146.

5. B. Malic, J. Bernard, J. Holc, M. Kosec, Strontium Doped $K_{0.5}Na_{0.5}NbO_3$ Based Piezoceramics, Ferroelectrics. 314 (2005) 149–156.

6. M.D. Maeder, D. Damjanovic, N. Setter, Lead free piezoelectric materials, J. Electroceramics. 13 (2004) 385–392.

7. G. Ferin, T. Hoang, C. Bantignies, H. Le Khanh, E. Flesch, A. Nguyen-dinh, Powering autonomous wireless sensors with miniaturized piezoelectric based energy harvesting devices for NDT applications, IEEE Int. Ultrason. Symp. (2015) 3–6.

8. I. Coondoo, N. Panwar, H. Maiwa, A.L. Kholkin, Improved piezoelectric and energy harvesting characteristics in lead-free $Fe_2O_3$ modified KNN ceramics, J. Electroceramics. 34 (2015) 255–261.

9. L. Besra, M. Liu, A review on fundamentals and applications of electrophoretic deposition (EPD), Prog. Mater. Sci. 52 (2007) 1–61.

10. M. Dolhen, A. Mahajan, R. Pinho, M.E. Costa, G. Trolliard, P.M. Vilarinho, Sodium potassium niobate ($K_{0.5}Na_{0.5}NbO_3$, KNN) thick films by electrophoretic deposition, RSC Adv. 5 (2014) 4698–4706.

11. A. Mahajan, R. Pinho, M. Dolhen, M.E. Costa, P.M. Vilarinho, Unleashing the full sustainable potential of thick films of lead-free potassium sodium niobate ($K_{0.5}Na_{0.5}NbO_3$) by aqueous electrophoretic deposition, Langmuir. 32 (2016) 5241–5249.

12. H. Mercier, B. Malič, H. Uršič, J. Hreščak, F. Levassort, D. Kuscer, Electrophoretic deposition and properties of strontium-doped sodium potassium niobate thick films, J. Eur. Ceram. Soc. 37 (2017) 5305-5313.

13. R. k. Bordia, R. Raj, Sintering Behavior of Ceramic Films Constrained by a Rigid Substrate, J. Am. Ceram. Soc. 68 (1985) 287–292.

14. G.W. Scherer, T. Garino, Viscous Sintering on a Rigid Substrate, J. Am. Ceram. Soc. 68 (1985) 216–220.

15. R.K. Bordia, A. Jagota, Crack Growth and Damage in Constrained Sintering Films, J. Am. Ceram. Soc. 76 (1993) 2475–2485.

16. F. Rubio-marcos, J.F. Fernández, Role of sintering time , crystalline phases and symmetry in the piezoelectric properties of lead-free KNN-modified ceramics, Mater. Chem. Phys. (2010).

17. X. Vendrell, J.E. García, F. Rubio-marcos, D.A. Ochoa, L. Mestres, J.F. Fernández, Exploring different sintering atmospheres to reduce nonlinear response of modified KNN piezoceramics, J. Eur. Ceram. Soc. 33 (2013) 825–831.

18. K.N. Li, X. Vendrell, L. Mestres, Optimization of the sintering conditions of the $[(K_{0.5}Na_{0.5})_{1-x}Li_x]NbO_3$ system, Phys. Procedia. 8(2010) 57–62.

19. N.M. Hagh, B. Jadidian, A. Safari, Property-processing relationship in lead-free (K, Na, Li) $NbO_3$ -solid solution system, J. Electroceramics. 18(2007) 339–346.

20. K. Kerman, M. Abazari, E.K. Akdo, A. Safari, Lead Free (K , Na)$NbO_3$ -based Piezoelectric Ceramics and Transducers, 17th IEEE Int. Symp. Appl. Ferroelectr. 3 (2008) 1–3.

21. J. Hreščak, B. Malič, J. Cilenšek, A. Benčan, Solid-state synthesis of undoped and Sr-doped $K_{0.5}Na_{0.5}NbO_3$: Study by thermal analysis and in situ high-temperature X-ray diffraction, J. Therm. Anal. Calorim. (2016).

22. International Centre for Diffraction Data. PDF-ICDD, PCPDFWin Version2.2. June 2001. Newtown Square; 2002. p. Newtown Square, PA.

23. R. Krimholtz, D.A. Leedom, G.L. Matthaei, New Equivalent Circuits for Elementary Piezoelectric Transducers, Electron. Lett. 6 (1970) 398–399.

24. A.R. Selfridge, Approximate material properties in isotropic materials, IEEE Trans. Sonics Ultrason. 32 (1985) 381–394.

25. A. Jagota, C.Y. Hui, Mechanics of sintering thin films — II. Cracking due to self-stress, Mech. Mater. 11 (1991) 221–234.

26. K.B. Singh, M.S. Tirumkudulu, Cracking in Drying Colloidal Films, Phys. Rev. Lett. 98 (2007) 218302.

27. J. Hreščak, G. Dražić, M. Deluca, I. Arčon, A. Kodre, M. Dapiaggi, T. Rojac, B. Malič, A. Bencan, Donor doping of $K_{0.5}Na_{0.5}NbO_3$ ceramics with strontium

and its implications to grain size, phase composition and crystal structure, J. Eur. Ceram. Soc. 37(2017) 2073-2082.

28. A.B. Haugen, F. Madaro, L. Bjørkeng, T. Grande, M. Einarsrud, Sintering of sub-micron $K_{0.5}Na_{0.5}NbO_3$ powders fabricated by spray pyrolysis, J. Eur. Ceram. Soc. 35(2015) 1449-1457.

29. A. Popovič, L. Bencze, J. Koruza, B. Malič, Vapour pressure and mixing thermodynamic properties of the $KNbO_3$ –$NaNbO_3$ system, RSC Adv. 5 (2015) 76249–76256.

30. J. Tellier, B. Malic, B. Dkhil, D. Jenko, J. Cilensek, M. Kosec, Crystal structure and phase transitions of sodium potassium niobate perovskites, Solid State Sci. 11 (2009) 320–324.

31. V.Y. Shur, A.A. Esin, D.O. Alikin, A.P. Turygin, A.S. Abramov, J. Hre, A. Bencan, B. Malic, A.L. Kholkin, V.Y. Shur, Ceramics dielectric relaxation and charged domain walls in (K ,Na) $NbO_3$ -based ferroelectric ceramics, 74101 (2017).

32. F. Levassort, J.-M. Gregoire, M. Lethiecq, K. Astafiev, L. Nielsen, R. Lou-Moeller, W.W. Wolny, High frequency single element transducer based on pad-printed lead-free piezoelectric thick films, in: IEEE International Ultrasonics Symposium, ( 2011) 848–851.